Mellado Romero, AM.; Borrachero Rosado, MV.; Soriano Martinez, L.; Paya Bernabeu, JJ.; Monzó Balbuena, JM. (2013). Inmobilization of Zn(II) in Portland cement pastes. Determination of microstructure and leaching performance. Journal of Thermal Analysis and Calorimetry. 112(3):1377-1389. doi:10.1007/s10973-012-2705-8.

Immobilization of Zn(II) in Portland cement pastes: Determination of microstructure and leaching performance

A. Mellado*, M.V. Borrachero, L. Soriano, J. Payá, J. Monzó

Instituto de Ciencia y Tecnología del Hormigón, ICITECH, Universitat Politècnica de València, Camino de Vera s/n, 46022 Valencia, Spain.

Abstract

The aim of this paper is to study the solidification/stabilization potential of cementitious matrices on the immobilization of Zn (II) before its disposal into the environment, by determining the mechanisms of interaction between the Zn (II) ions and the binder. The results of structural and mineralogical characterization of cement pastes formed with different amounts of immobilized Zn (II) ions are presented and the study includes results from thermogravimetric analysis (TG), scanning electron microscopy (SEM), X-Ray diffraction (XRD) and leaching performance. Zn (II) ions delay hydration reaction of Portland cement due to the formation of $CaZn_2(OH)_6 \cdot 2H_2O$ mainly, as well as $Zn_5(CO_3)_2(OH)_6$, and $Zn(OH)_2$ and $ZnCO_3$ in minor proportion. Correlations between total mass loss in TG analysis and leached Zn (II) ions in long term curing pastes have been obtained. This result is important because, in a preliminary approach from a thermogravimetric analysis on an early-aged cement paste containing Zn (II), it could be possible to perform an estimation of the amount of Zn (II) ions that could be leached, thus avoiding costly and time-consuming tests.

Keywords

Zn (II), immobilization, cement, leaching, thermogravimetry.

1. Introduction.

Thermal Analysis is a well-established set of techniques for obtaining qualitative and quantitative information about the effects of various heat treatments on materials of all kinds, including new chemical compounds, plastics, ceramics, alloys, construction materials, minerals, foods and medicines. Heating is performed under strictly controlled conditions and can reveal changes in structure and other important properties of the material being studied. Such studies are of great practical importance in the use of materials [1]. In the literature reviewed, there are many examples of applications that this technique has on the characterization of cementitious materials. Perraki et al. [2] studied the sintering and hydration processes of a modified raw mixture.

Thermogravimetry (TG) and derivative thermogravimetry (DTG) were used to analyze the early stages of hydration of a high-initial strength and sulphate resistant Portland cement within the first 24 h of setting at different water/cement (W/C) mass ratios [3]. The results show that a significant part of the hydration process occurs within the first 14 h of setting and at 24 hours the highest hydration degree occurs in the case of the highest initial water content of the paste assayed.

Portland cement hydration has been also investigated by emanation thermal analysis (ETA), based on the application of radon atoms as radioactive indicators. [4]. This method enables to characterize continuously changes in the microstructure of the cement paste at selected temperatures.

* Corresponding author. Tel.: +34 96 3879564; fax: +34 96 3877569.
E-mail address: amellado@cst.upv.es (A. Mellado).

Zhang and Ye [5] have studied the dehydration kinetics data of cement paste at different heating rates by thermogravimetry. When cement paste is exposed to high temperature, the dehydration of cement paste leads to not only the decline in strength, but also the increased pore pressure in the paste.

In field structures affected by fire, the temperature progress through the material. The progression of temperature in the concrete material can be determined by simultaneous differential thermal analysis and thermogravimetry. Also, the analysis of the behaviour of concrete in real concrete, by different techniques, permits the corroboration of the hypothesis of cover calculation. In a recent paper published by Menendez et al. [6], the analysis of concrete exposed to a very severe fire has been showed in order to corroborate the calculus hypothesis and to determine the progression of the temperature inside the affected structure. In this study, the potentiality of the thermal instrumental techniques has been studied to determine the situation of the concrete exposed to fire. These results can be used to calculate the residual strength of the concrete structural elements. Also, other auxiliary techniques have been used to have some supplementary information about the situation of the concrete exposed to fire. The results are based in concrete samples from a real fire in the Windsor Building in Madrid.

Thermogravimetrical analysis can be used for monitoring carbonation of cementitious materials [7]. The carbonation reaction is a crucial phenomenon from the point of view of structure durability and also for cement-based materials sustainability.

One of the most widely used technologies for safe immobilization of wastes containing heavy metals before their disposal into the environment is cement solidification/stabilization (S/S), although those wastes of metal confined in cement matrices can interfere with their hydration processes during solidification [8] even if they are at trace level [9]. In fact, a decrease in mechanical strength in S/S products containing heavy metals [10] has been found. The progress of hydration can be monitored with heat evolution measurements and calorimetric results are considered indicators of the degree of hydration [11].

Portland cement blended with calcium carbonate is being used to study the solidification/stabilization (S/S) of a Brazilian tanning waste which arises from leather production [12]. Chromium is the element of greatest concern in this waste, but the waste also contains a residual organic material. Thermogravimetry (TG) and derivative thermogravimetry (DTG) are used to identify and quantify the main hydrated phases present in the pastes.

Other authors have studied two catalyst wastes from polyol production, which were considered hazardous due to their respective high concentration of nickel and aluminum contents respectively [13]. The paper presents the study carried out to avoid environmental impact, of the simultaneous solidification/stabilization of both catalyst wastes with type II Portland cement with the use of non-conventional differential thermal analysis. This technique not only allows to monitor the initial stages of cement hydration to evaluate the accelerating and/or delaying effects on the process due to the presence of the wastes but also to identify the steps where the changes occur.

Thermogravimetric analysis (TG) was also applied to the characterization of pozzolanic reaction in mortars containing the supplementary cementitious materials (SCMs): pitchstone fines and fly ash as partial replacements of Portland cement (PC) [14]. TG was used to determine the proportion of calcium hydroxide (CH) present after the hydration of the Portland cement by observing the dehydration of the CH present in the blended PC-SCM mortars.

Zn (II) is known to interact chemically with cement grains during hydration. Binding mechanisms of this element with cement have been widely studied. Tommaseo and Kersten [15] propose that the uptake of Zn (II) by calcium silicate hydrate (C-S-H) takes a three-step mechanism: (i) adsorption of Zn (II) ions and surface precipitation of calcium zincate

on C-S-H precursor gel due to the highly alkaline environment, (ii) disintegration of the metastable zincate phase upon polymerization of the C-S-H phase, and (iii) solid-state diffusion of Zn (II) ions from external to internal sites and fixation at lattice positions inside the maturating and thereby recrystallizing C-S-H structure.

The formation of an impermeable layer of crystalline calcium hydroxyzincate, $CaZn_2(OH)_6 \cdot 2H_2O$, or amorphous zinc hydroxide, $Zn(OH)_2$, at the surface of C_3S and C_2S grains accounts for the inhibition of the binder hydration. The role of Zn (II) in this inhibition process has been confirmed by its enrichment in the hydrated layer surrounding the unhydrated grains [16].

Moulin et al. suggested that Zn (II) retention by C-S-H can be attributed to the linkage of ions to tetrahedral silicates chains, whereas its retention by calcium aluminate is essentially controlled by precipitation of calcium hydroxyzincate [17].

Ziegler et al. observed that the incorporation of Zn (II) in the interlayer of C-S-H or sorption to internal surfaces of crystals appear to be the most probable mechanisms for the observed Zn (II) sorption to C-S-H [18]. For high Zn (II) concentrations, the precipitation of $Zn(OH)_2$ was observed at pH<12 and calcium zincate at pH>12.

A study reveals that Zn (II) has detrimental effects on the hydration of C_3S at early curing ages [19] with the inhibiting its hydration due to the formation of hydroxyzincate. This fact was demonstrated by the absence of the $Ca(OH)_2$ in samples containing Zn (II) because of the formation of hydroxyzincate.

According to a review published by Chen et al. [20], there are many contradictory speculations about the mechanisms dominating the fixation of heavy metals in hydrated cement matrix. In fact, these authors have published a paper about the influence of Zn (II), Pb (II), Cu (II) and Cr (III) on C_3S hydration [21]. It proves the hydration acceleration of C_3S by the heavy metals except Zn (II), whereas all of them retarded the precipitation of Portlandite due to the reduction of pH resulting from the hydrolysis of heavy metals ions during C_3S hydration. $CaZn_2(OH)_6 \cdot 2H_2O$ was identified in analyzed samples.

The degree of effectiveness of the S/S products can be defined by leach strength [10]. For example, Fernandez-Olmo et al. [22] showed that ZnO delays the setting time strongly; it also decreases the unconfined compressive strength of the final product at short curing ages, but this effect decreases with ageing. In respect to the leaching performance, a study carried out by same authors shows that the immobilization of Zn (II) as oxide in Portland cement is poor; this compound behaves similarly to their amphoteric hydroxides [23]. The leaching of Zn (II) ions in water is also influenced by the composition of the product: several compounds may show an influence on the leaching of each individual ion.

A paper published by Cappuyns et al. [24] discusses the use of pH_{stat} leaching tests as a tool to assess the potential mobilization of heavy metals from waste materials. They found 5 different types of heavy metal leaching behaviour. Zn (II) belongs to type 2: elements that display an initially rapid release, followed by a slow but substantial release in the final stage of the test. This performance indicates the dissolution of poorly stable solid phases.

The aim of this paper is to study the S/S potential of cementitious matrices on Zn (II) immobilization. Additional results of structural and mineralogical characterization of cement pastes formed with different amounts of Zn (II) ions immobilized are also presented. The study includes results from thermogravimetric analysis, scanning electron microscopy, X-Ray diffraction and leaching performance.

2. Materials and methods.

In the preparation of cement pastes, it was used Spanish ordinary Portland cement (CEM I-52.5-R) supplied by Lafarge-Asland company (Sagunto, Valencia).

The mixture formulations of this study were prepared as follows: an appropriate amount of Zn (II) ions, from the soluble salt $Zn(NO_3)_2 \cdot 6H_2O$ (from Panreac, quality reagent), was weighed to obtain Zn (II) ion/binder percentages of 0.1, 1, 2.5, 5 and 10 %. Salts were dissolved in distilled water previously to mix with the cement. The water/cement ratio was 0.5 in all cases. After mixing, pastes were stored in sealed plastic bottles and then left in a curing room at 20 ºC until the day of testing; then, they were pulverized by manual grinding in an agate mortar; the hydration was stopped with acetone and samples were dried at 60 ºC for half an hour. Selected curing times were 7 hours and 1, 3, 7, 14 and 28 days.

Thermogravimetric analysis (TG) was performed in a Mettler-Toledo TGA850 thermobalance with a horizontal furnace. It is equipped with an ultramicrobalance that has a resolution of 0.1 μg. Aluminum crucibles of 100 μl were used, having a sealable lid with a pin hole to obtain the water vapour self-generated atmosphere [25]. The gas flow for the surrounding atmosphere was 75 ml/min of nitrogen. The heating rate was 10 ºC/min in the temperature range 35-600 ºC, and the mass of the sample for thermogravimetric analysis was in the range 40-45 mg.

After more than 100 days of curing, the microstructure of hardened samples was observed by scanning electron microscopy (SEM) by using a JEOL JSM-6300 equipped with energy dispersive LINK-ISIS micro analyzer from Oxford Instruments.

XRD studies were carried out on some powdered samples (particle size < 125 μm), by using a Philips PW 1710 Based X-Ray diffractometer.

Leaching studies were carried out with an automatic titration system 775 Dosimat from Metrohm coupled with a pH transmitter from LabProcess, model DO 9765T. 1 g of powdered sample (particle size < 125 μm, curing time > 270 days), previously dried at 60 ºC for half an hour and stored in a dried atmosphere, was weighed and placed in a beaker; then 50 ml of distilled water was added (L/S ratio was 50). The sample was maintained in suspension with the help of a magnetic stirrer device with the rod spinning at 300 rpm. After 10 min of stirring, the test started with the addition of HNO_3 1 M from the dispenser at a flow rate of 4 ml/min, until the pH reached the selected value. The assay was finished after 1 hour of maintenance at this pH, by the automatic addition to the acid from the titrator; added HNO_3 volumes were recorded during the entire test. Selected pH values for tests were 7, 4 and 2.

Resulting suspensions were filtered at a reduced pressure with paper filters of pore size of 11 μm and eluates were conserved until the analysis by adjusting pH to 2, in order to prevent changes.

Determination of concentration of Zn (II) ions in eluates was carried out with a Merck photometer SQ 118 according to Spectroquant zinc cell test 14832.

A synthesis of calcium hydroxyzincate was made to have a reference material to confirm their structural characteristics by XRD and TG studies. For this purpose, the method of Wang et al. [26] was used although it had some slight modifications. Solid reagents ZnO (from Guinama, USP reagent) and $Ca(OH)_2$ (from Panreac, quality reagent), in a 2/1 molar ratio, were added to a well-sealed reaction vessel containing distilled water and connected to a thermostatic bath (P-Selecta, Ultraterm model) at a controlled temperature of 75 ºC. The mixture was maintained in constant stirring

during 48 hours. After reaction, the solution was left until reaching room temperature (about 12 hours) and afterwards, it was filtered and dried at 60 ºC.

3. Results and discussion.

3.1. X-Ray studies.

In Figure 1 **a**, it is shown the XRD pattern of calcium hydroxyzincate synthesized as reference material. The peaks correspond to the compound $CaZn_2(OH)_6 \cdot 2H_2O$, and small impurities of zincite (ZnO) and calcite ($CaCO_3$) are also identified [21].

In Table 1, mineralogical phases identified by XRD for control paste (only cement) and with 0.1, 1 and 10 % Zn (II) pastes are shown. It is necessary to point out that the diffractograms show the major peaks corresponding to calcite, and indicate the presence of filler in the cement and that natural carbonation occurred during the sample preparation and storage, as well. Other major peaks identified in all diffractograms are those relating to β-C_2S. Additionally, traces of hydrated calcium silicates of gyrolite type are detected, according to bibliographic data [27].

Figure 1 **b** shows the XRD of control and 10 % Zn (II) pastes at 28 days' curing time. In the control paste, the peaks due to Portlandite are clearly observed. The intensity of these peaks is greatly reduced in the paste with 0.1 % Zn (II) and it is no longer detected in the paste with 1 % Zn (II) (Table 1) nor 10 % Zn (II) paste (Figure 1 **b**). On the contrary, in pastes containing Zn (II) ions, it has been possible to detect the peaks of the calcium hydroxyzincate compound ($CaZn_2(OH)_6 \cdot 2H_2O$) (Table 1) [21, 26]. In addition, for the paste with 10 % Zn (II), some trace amount of β-$Zn(OH)_2$ has also been detected.

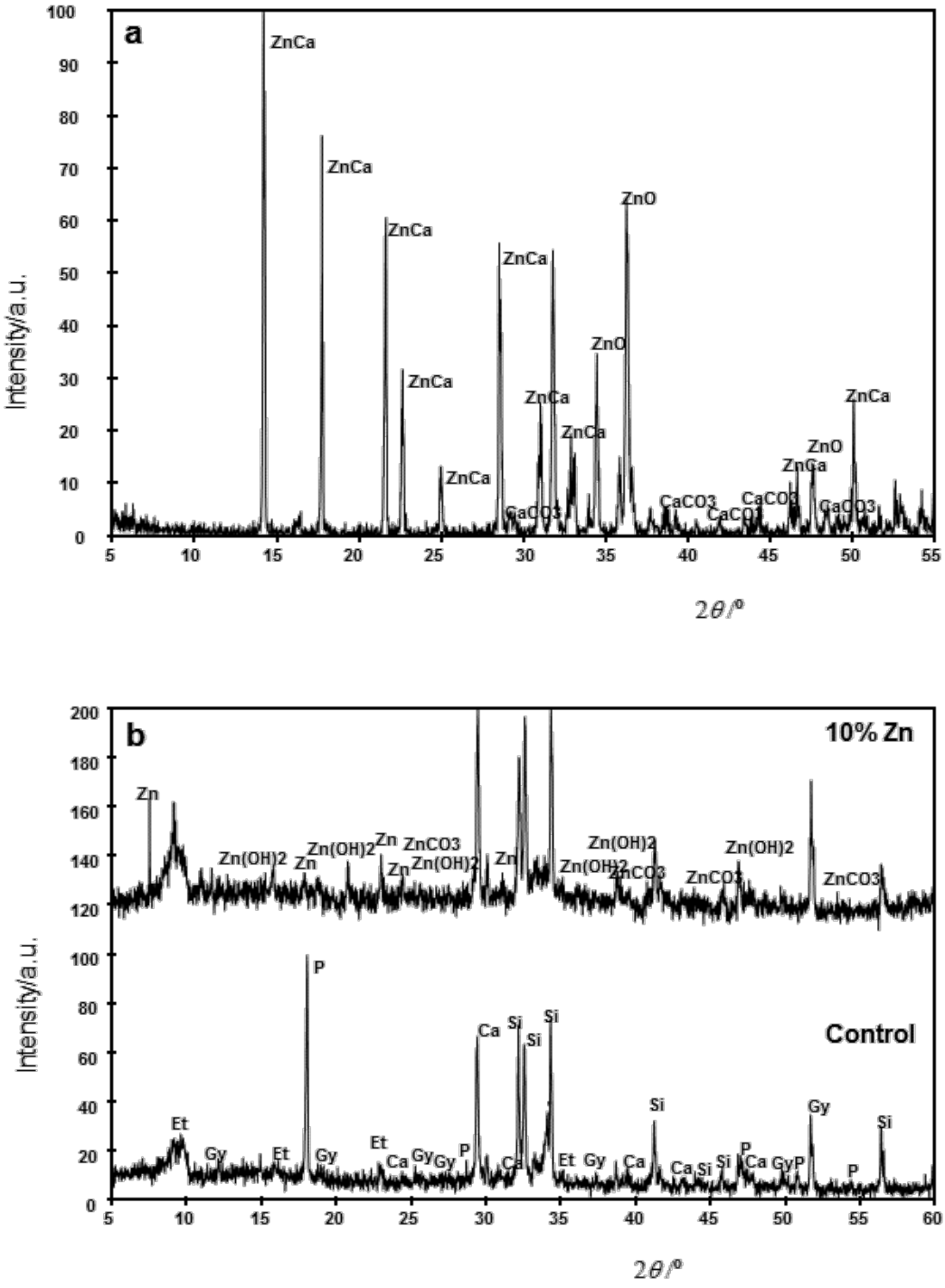

Fig. 1 XRD of **a** calcium hydroxyzincate synthesized (ZnCa is calcium hydroxyzincate, $CaZn_2(OH)_6{\cdot}2H_2O$; ZnO is zincite; CaCO3 is calcite, $CaCO_3$) and **b** control and 10 % Zn (II) pastes at 28 days' curing time (P is Portlandite, $Ca(OH)_2$; Ca is calcite, $CaCO_3$; Si is dicalcium silicate, β-Ca_2SiO_4; Et is ettringite, $Ca_6Al_2(SO_4)_3(OH)_{12}{\cdot}26H_2O$; Gy is Gyrolite, $Ca_8Si_{12}O_{30}(OH)_4{\cdot}7H_2O$; Zn is calcium hydroxyzincate, $CaZn_2(OH)_6{\cdot}2H_2O$; Zn(OH)2 is Zinc hydroxide, β-$Zn(OH)_2$; and ZnCO3 is Smithsonite, $ZnCO_3$).

	Control	0.1 % Zn (II)	1 % Zn (II)	10 % Zn (II)
Calcite/$CaCO_3$	***	***	***	***
Ettringite/$Ca_6Al_2(SO_4)_3(OH)_{12}\cdot 26H_2O$	**	**	**	**
Portlandite/$Ca(OH)_2$	***	*		
Calcium silicate/β-$CaSiO_4$	***	***	***	***
Calcium hydroxyzincate/$CaZn_2(OH)_6\cdot 2H_2O$		*	*	**
Gyrolite/$Ca_8Si_{12}O_{30}(OH)_4\cdot 7H_2O$	*	*	*	*
Zinc hydroxide/β-$Zn(OH)_2$			*	**
Smithsonite/$ZnCO_3$				**
***/major compound **/minor compound */trace compound				

Table 1 Mineralogical phases identified by XRD for control paste and 0.1, 1 and 10 % Zn (II) pastes.

3.2. Thermal analysis.

3.2.1. General aspects.

We have observed a strong delay in the initial hardening in the pastes containing Zn (II) ions, which is in accordance with data from the literature [28]. The highest retard effect on the hydration of cement was observed for 2.5, 5 and 10 % Zn (II) pastes (after 28 days of curing, the mass remains a little bit soft).

In Figure 2, TG and first derivative (DTG) curves for the control paste at 28 days' curing time are represented. Three main zones can be identified in the DTG curve [25]: Zone (1) (100-180 ºC range) is attributed to overlapped peaks of the dehydration of ettringite (AF_t) and C-S-H; zone (2) (180-240 ºC range) corresponds to the dehydration of calcium aluminate and calcium aluminosilicate hydrates; and zone (3) (520-580 ºC range) is due to the dehydration of Portlandite.

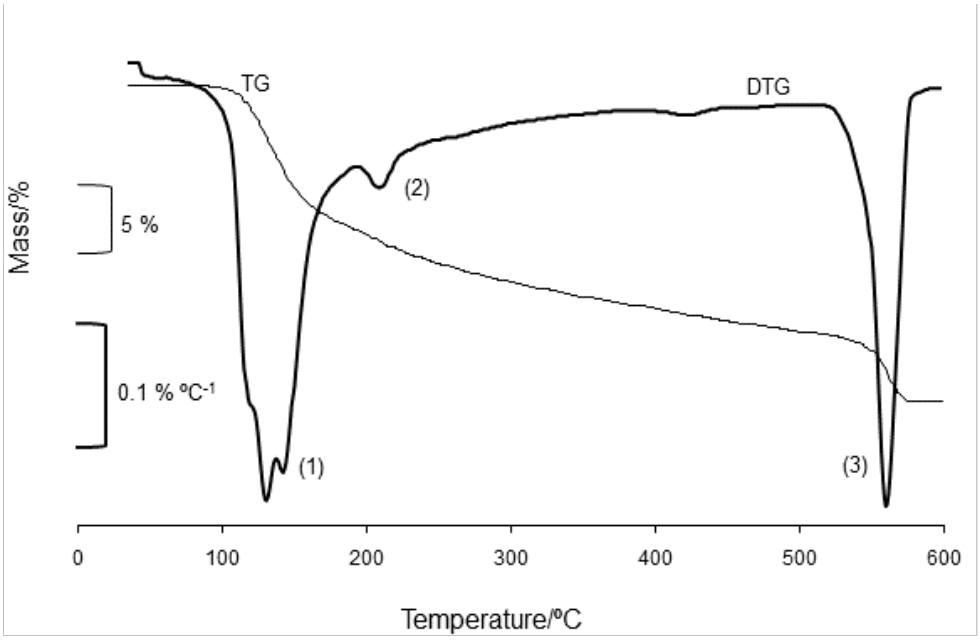

Fig. 2 TG and DTG curves of control paste at 28 days' curing time.

In order to detect the presence of $CaZn_2(OH)_6 \cdot 2H_2O$, a previous thermogravimetric analysis was performed to the sample synthesized as reference [26] for Zn (II) containing pastes. Figure 3 shows their TG and DTG curves. In the DTG curve, three peaks are detected (first and second peaks are overlapped), which correspond to a three-stage decomposition of hydrated calcium hydroxyzincate [21]:

$$CaZn_2(OH)_6 \cdot 2H_2O \rightarrow CaZn_2(OH)_6 + 2\,H_2O \quad (1)$$

$$CaZn_2(OH)_6 \rightarrow 2\,ZnO + Ca(OH)_2 + 2\,H_2O \quad (2)$$

$$Ca(OH)_2 \rightarrow CaO + H_2O \quad (3)$$

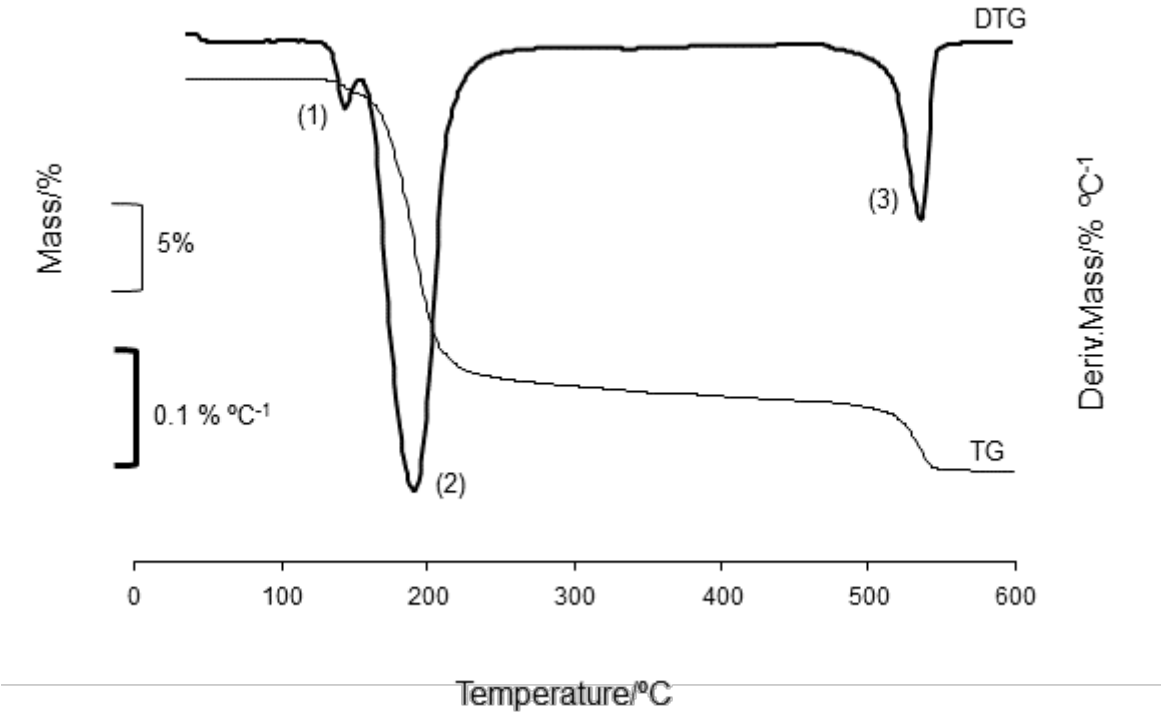

Fig. 3 TG and DTG curves of $CaZn_2(OH)_6 \cdot 2H_2O$, synthesized.

In table 2 are shown, the thermogravimetric data (mass losses and peak temperatures). With stoichiometric calculations, we can deduce that the purity of synthesized compound is 89.7 %.

M_T/% 35 – 600 ºC	M_1/% 140 – 350 ºC	M_2/% 489 – 550 ºC	M_1/ºC Peak 1	M_2/ºC Peak 2	M_3/ºC Peak 3	% $CaZn_2(OH)_6 \cdot 2H_2O$
25.34	20.11	5.23	144	181	537.5	89.7

Table 2 Thermogravimetric data of $CaZn_2(OH)_6 \cdot 2H_2O$, synthesized.

Figure 4 shows the comparison between DTG curves of control sample and that one containing 1 % of Zn (II), at 3 days' curing time. In the DTG curve for Zn (II) paste, the absence of Portlandite decomposition process is observed. This fact is related to bibliographic data, which confirm that the presence of Zn (II) ions produces a delay of Portland cement setting. Also, two new peaks centered at 178 and 289 ºC respectively are detected, whose origin will be discussed in further sections.

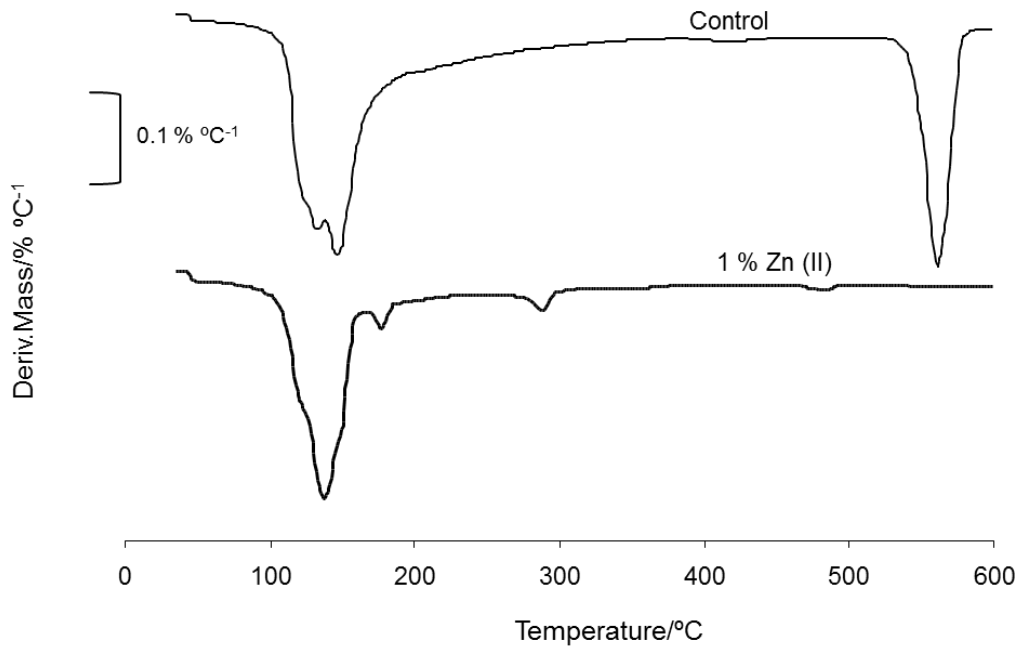

Fig. 4 DTG curves of control and 1 % Zn (II) pastes at 3 days' curing time.

3.2.2. Influence of Zn (II) content in cement pastes.

Table 3 shows the main significant values taken from TG and DTG curves of control and 0.1 % Zn (II) pastes, cured at different ages (7 and 24 hours, 3, 7, and 28 days), being:

M_T (35-600 ºC): Total mass loss in the 35-600 ºC temperature range,

M_{CH} (480-580 ºC): Mass loss in the 480-580 ºC temperature range, due to the dehydration of Portlandite (CH),

$\%\ CH_p$: Portlandite percentage present in the paste, calculated with the following equation:

$$\%\ CH_p = \frac{M_{CH}}{18} \cdot 74 \qquad (4)$$

(where 74 and 18 correspond to the molecular mass of CH and water, respectively),

M_H: Mass loss due to the water release in the decomposition except Portlandite, which has been calculated with the following equation:

$$M_H = M_T - M_{CH} \qquad (5)$$

Paste	Curing time	M_T 35 – 600 ºC	M_{CH} 480 – 580 ºC	% CH_p	M_H	Significant DTG peaks due the Zn (II) incorporation/ºC
Control	7 hours	8.07	1.20	4.93	6.87	-
0.1 % Zn (II)		2.93	0.05	0.23	2.91	183/283
Control	1 day	13.48	2.52	10.37	10.96	-
0.1 % Zn (II)		14.27	2.31	9.52	11.95	180/290
Control	3 days	17.66	3.29	13.54	14.36	-
0.1 % Zn (II)		17.57	3.11	12.79	14.46	-
Control	7 days	20.40	3.61	14.85	16.79	-
0.1 % Zn (II)		20.27	3.46	14.24	16.81	-
Control	28 days	21.63	3.86	15.86	17.77	-
0.1 % Zn (II)		20.80	3.69	15.16	17.11	-

Table 3 Values obtained from TG and DTG curves of control and 0.1 % Zn (II) pastes, cured at 7 and 24 hours and 3, 7 and 28 days.

In Figure 5, DTG curves of the control and 0.1 % Zn (II) pastes to 7 hours (**a**) and 28 days (**b**) are shown. It is observed a reduction in the peak due to the decomposition of Portlandite in the paste with Zn (II) ions, which is greater for short curing ages. This fact is due to a delay in the setting paste. From 1 day curing time, no peaks have been found due to the presence of Zn (II) compounds. This delay is clearly shown in Figure 6, where the Portlandite percentage present at the pastes, calculated with the equation (4), as a function of curing time for control and 0.1 % Zn (II) pastes is represented. The percentage of decrease in Portlandite, *% CH (R)*, in the 0.1 % Zn (II) paste respect to the control is plotted, according to the following equation:

$$\%\ CH\ (R) = \frac{\%\ CH_p\ (\text{control}) - \%\ CH_p\ (\text{Zn (II) 0.1 \%})}{\%\ CH_p\ (\text{control})} \cdot 100 \qquad (6)$$

% CH_p (control): Portlandite percentage present at the control paste,

% CH_p (Zn (II) 0.1 %): Portlandite percentage present at the 0.1 % Zn (II) paste,

% CH (R): Percentage of decrease in Portlandite.

At seven hours' curing time, the reduction in the amount of Portlandite in the paste with Zn (II) is 95.91 %, whereas this percentage decreased with curing time, thus being 4.4 % at 28 days' curing time.

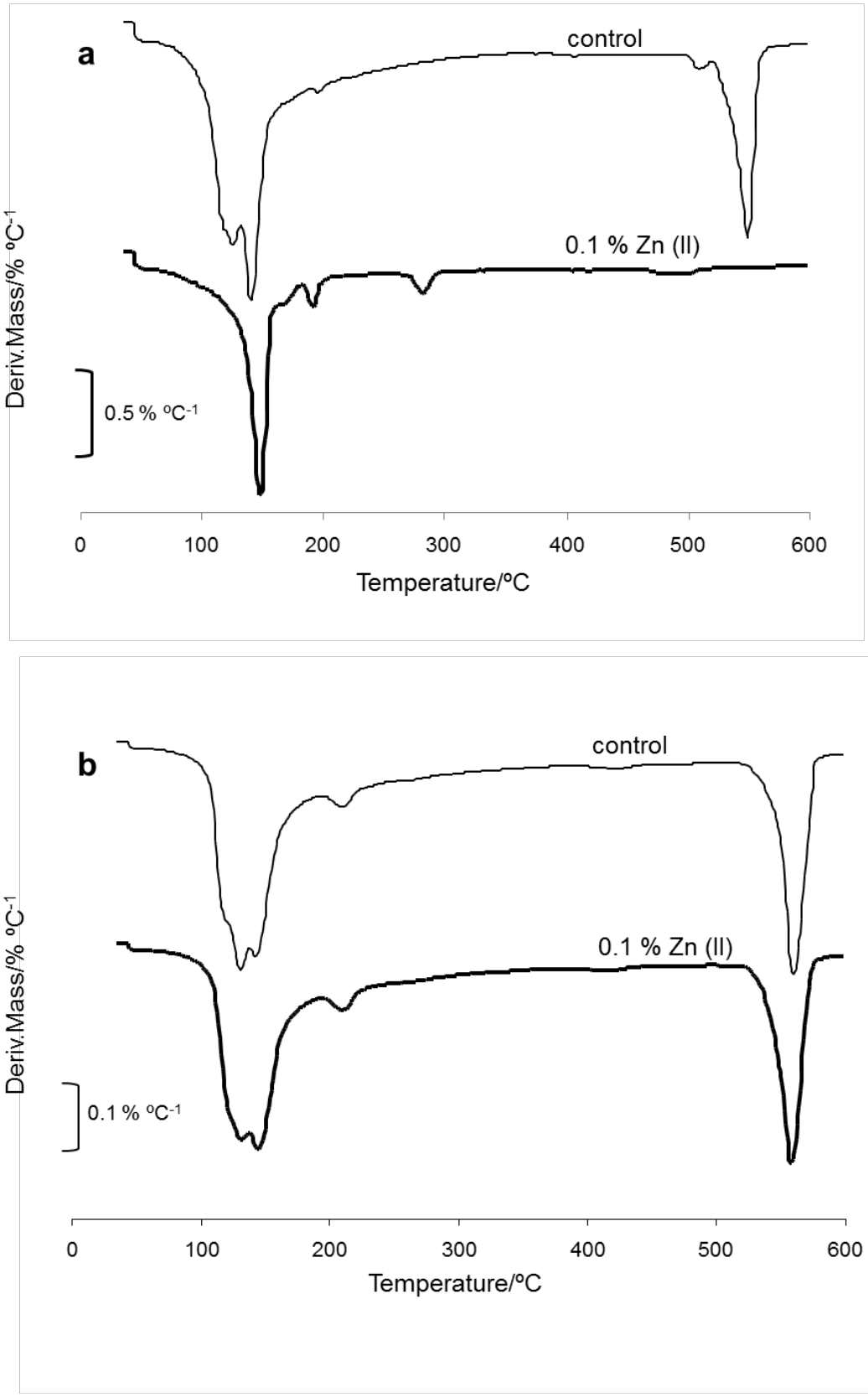

Fig. 5 DTG curves of control and 0.1 % Zn (II) pastes cured at **a** 7 hours and **b** 28 days.

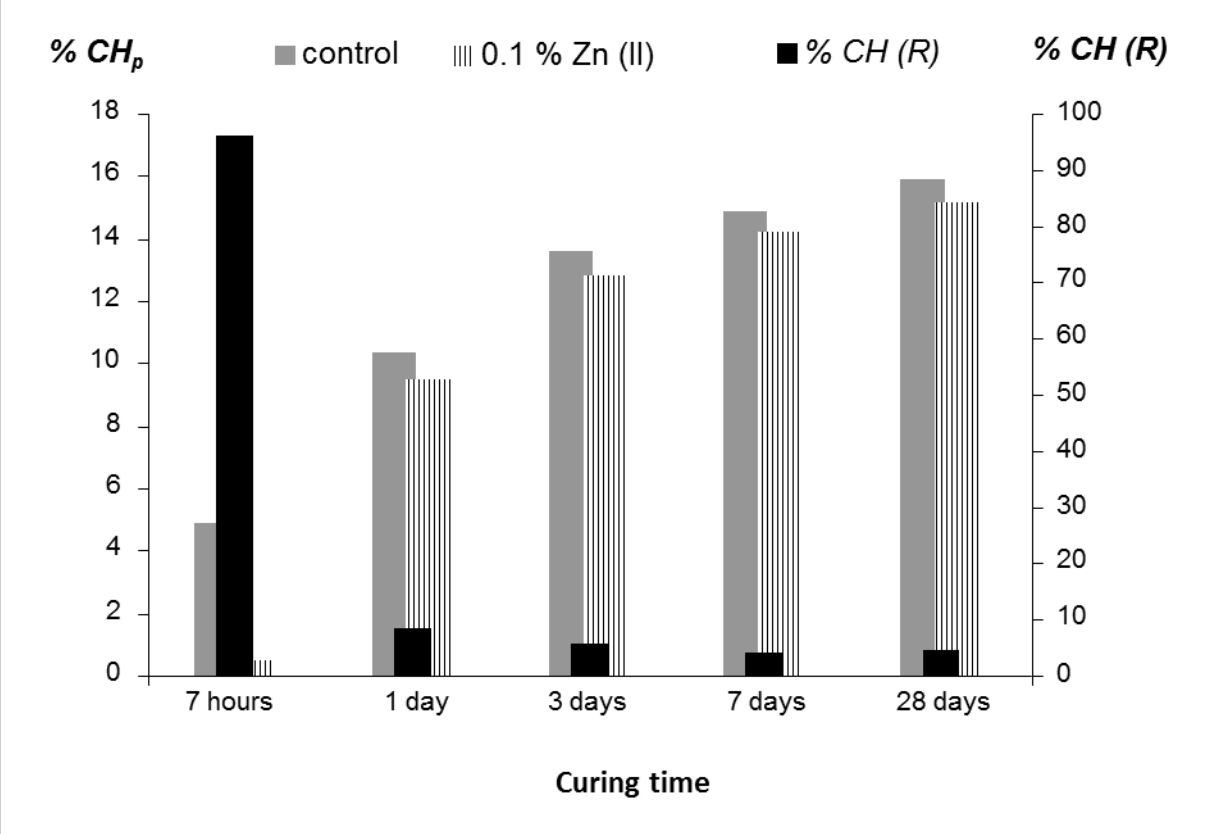

Fig. 6 Percentage of Portlandite, *% CH_p*, present at the control and 0.1 % Zn (II) pastes and decrease in the percentage of Portlandite, *% CH (R)*, in the 0.1 % Zn (II) paste in respect to the control paste versus curing time.

In Table 4, the main significant values from TG and DTG curves for 1 % Zn (II) paste are given and in Figure 7, DTG curves of pastes with 1 % Zn (II) at different curing times (7 hours, 3, 7 and 28 days) are plotted. At short curing times (7 hours, 1 and 3 days) the appearance of a new peak centered at 180 ºC has been observed, it is assigned to the decomposition of hydrated calcium hydroxyzincate, according to equation (2). In addition, a peak detected in the temperature range 270-290 ºC is attributed to the decomposition of a basic Zn (II) carbonate: the hydrozincite [29, 30], according to the equation (7):

$$Zn_5(CO_3)_2(OH)_6 \rightarrow 5\,ZnO + 2\,CO_2 + 3\,H_2O \qquad (7)$$

In the temperature range 480-500 ºC, the process of dehydration of calcium hydroxide is not observed, which shows that there is a significant delay in the setting process.

At longer curing time (7 and 28 days) (Figure 7) the presence of Portlandite in the paste seems to occur, although it is difficult to quantify because the decomposition peak is overlapped with the peak, due to the process of decarbonation of Zn (II) carbonate (480-502 ºC range) (table 4), [31]:

$$ZnCO_3 \rightarrow ZnO + CO_2 \qquad (8)$$

For these curing times, the peak attributed to the presence of hydrozincite (270-300 ºC range) is also detected. However, no peaks were observed due to the presence of hydrated calcium hydroxyzincate, which had been detected in the pastes cured at shorter times (table 4 and figure 8).

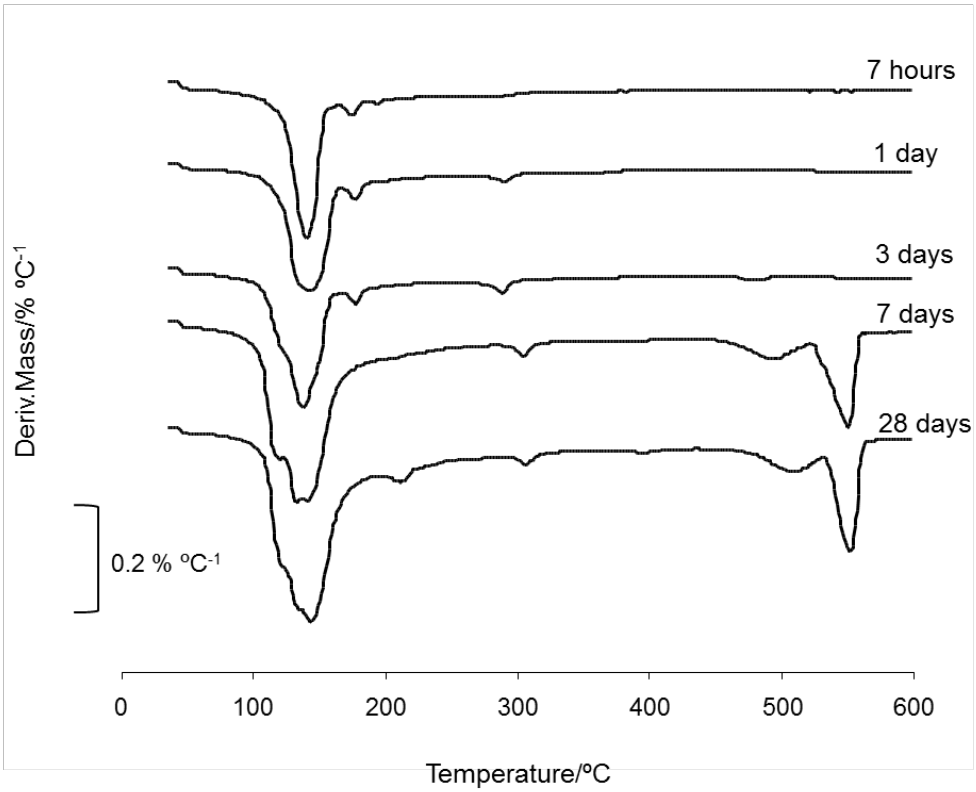

Fig. 7 DTG curves of 1 % Zn (II) pastes at several curing times.

Curing time	M_T 35 – 600 ºC	M_{CH} 480 – 580 ºC	% CH_p	M_H	Significant DTG peaks due the Zn (II) incorporation/ºC
7 hours	6.73	nd	-	6.73	178
1 day	7.77	nd	-	7.77	180/290
3 days	8.13	nd	-	8.13	178/289
7 days	19.84	1.83*	7.52	17.00	304/494
28 days	22.70	1.86*	7.66	19.60	306/510
nd/not determined */estimated values because of peak overlapping by decomposition of $ZnCO_3$					

Table 4 Thermogravimetric data for 1 % Zn (II) pastes at several curing times.

The pastes with higher amounts of Zn (II) ions (2.5 and 5 %) show a larger number of peaks (Table 5 and Figure 8). There are peaks previously detected in the pastes with 1 % of Zn (II) ions: a peak centered at 180 ºC attributed to the decomposition of hydrated calcium hydroxyzincate and a peak in the range 270-300 °C attributed to the presence of hydrozincite.

In the paste with 5 % Zn (II) ions at 7 and 28 days' curing time, a new peak in the DTG curve in the range 340-370 ºC is detected, which has been assigned to the decomposition of the zinc hydroxide, $Zn(OH)_2$ [31].

In the temperature range 480-530 ºC, a broad peak of low intensity is observed. In the 2.5 % Zn (II) paste this peak presents low intensity and could be due to the overlapping of decomposition processes of $Ca(OH)_2$ and $ZnCO_3$.

In the 5 % Zn (II) paste, the broad peak is more important and, probably, it could also have been produced by the incorporation of calcium hydroxyzincate in the interlayer structure of C-S-H [27]; thus the Portlandite formed is adsorbed on the surface of these silicates and it presents a more amorphous character, which may explain the wider temperature range of decomposition.

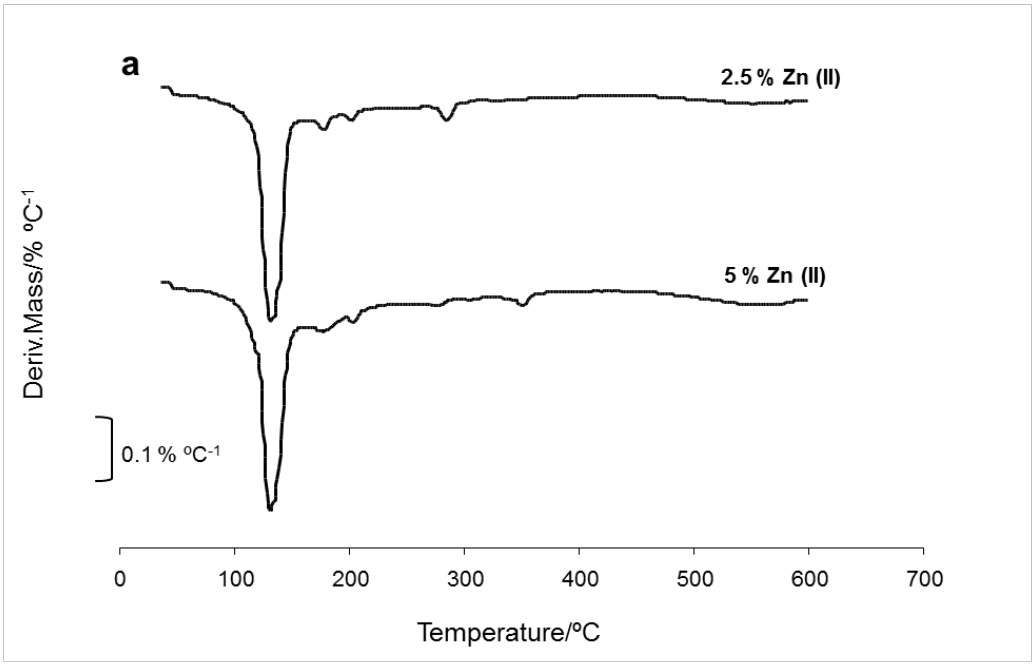

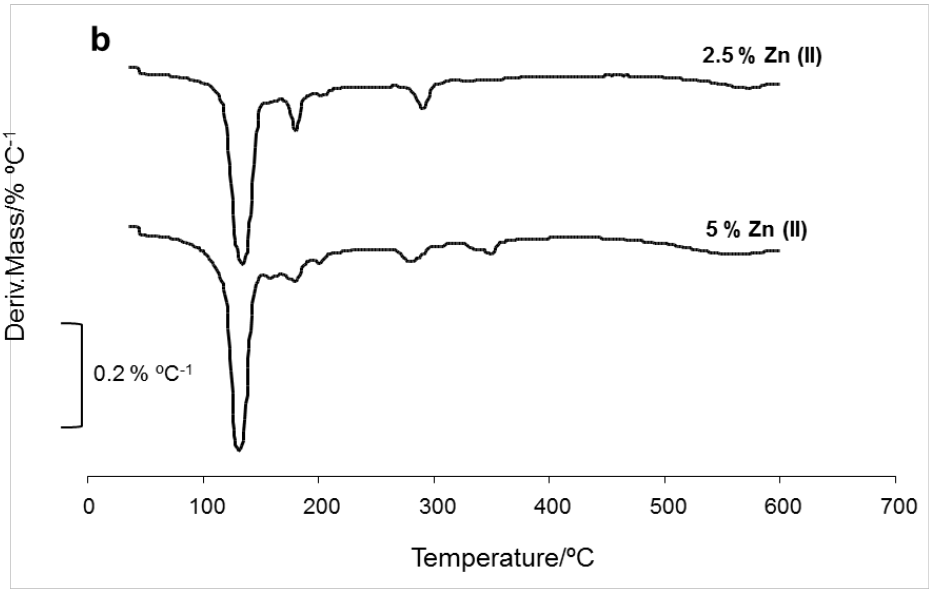

Fig. 8 DTG curves for 2.5 and 5 % Zn (II) pastes at **a** 7 hours and **b** 7 days' curing time.

Paste	Curing time	M_T 35 – 600 ºC	M_{CH} 480 – 580 ºC	% CH_p	M_H	Significant DTG peaks due the Zn (II) incorporation/ºC
2.5 % Zn (II)	7 hours	8.78	nd	-	8.78	180/285
5 % Zn (II)		10.58	nd	-	10.58	181/279/351/broad peak
2.5 % Zn (II)	1 day	9.55	nd	-	9.55	180/287
5 % Zn (II)		11.35	nd	-	11.35	180/276/347/broad peak
2.5 % Zn (II)	3 days	10.13	nd	-	10.13	180/289
5 % Zn (II)		12.11	nd	-	12.11	180/282/350/broad peak
2.5 % Zn (II)	7 days	10.57	nd	-	10.57	181/290/broad peak
5 % Zn (II)		13.00	nd	-	13.00	180/280/349/broad peak
2.5 % Zn (II)	28 days	11.10	nd	-	11.10	301/447/broad peak
5 % Zn (II)		13.58	nd	-	13.58	180/285/350/broad peak
nd/not determined						

Table 5 Calculated values from TG and DTG curves of 2.5 and 5 % Zn (II) pastes, cured at 7 and 24 hours and 3, 7 and 28 days.

The last process can be better identified in pastes containing 10 % Zn (II). In table 6, thermogravimetric data are shown and, in figure 9, TG and DTG curves of 10 % Zn (II) paste at 28 days of curing are plotted. In the DTG curve, the peak centered at 180 ºC is very intense (hydrated calcium hydroxyzincate), and the peak centered at 350 ºC is also clearly observed, attributed to the decomposition of zinc hydroxide, $Zn(OH)_2$.

The broad peak observed in pastes with lower content of Zn (II), 2.5 and 5 % Zn (II), is now fully defined in the temperature range 450-600 ºC due to the process of adsorption of calcium hydroxide, which had been discussed previously.

Curing time	M_T 35 – 600 ºC	M_{CH} 480 – 580 ºC	% CH_p	M_H	Significant DTG peaks due the Zn (II) incorporation/ºC
7 hours	12.15	nd	-	12.15	175/337/broad peak
1 day	12.90	nd	-	12.90	173/345/broad peak
3 days	14.88	nd	-	14.88	171/349/broad peak
7 days	16.06	nd	-	16.06	170/351/broad peak
28 days	18.42	nd	-	18.42	169/358/broad peak
nd/not determined					

Table 6 Thermogravimetric data of 10 % Zn (II) pastes at several curing times.

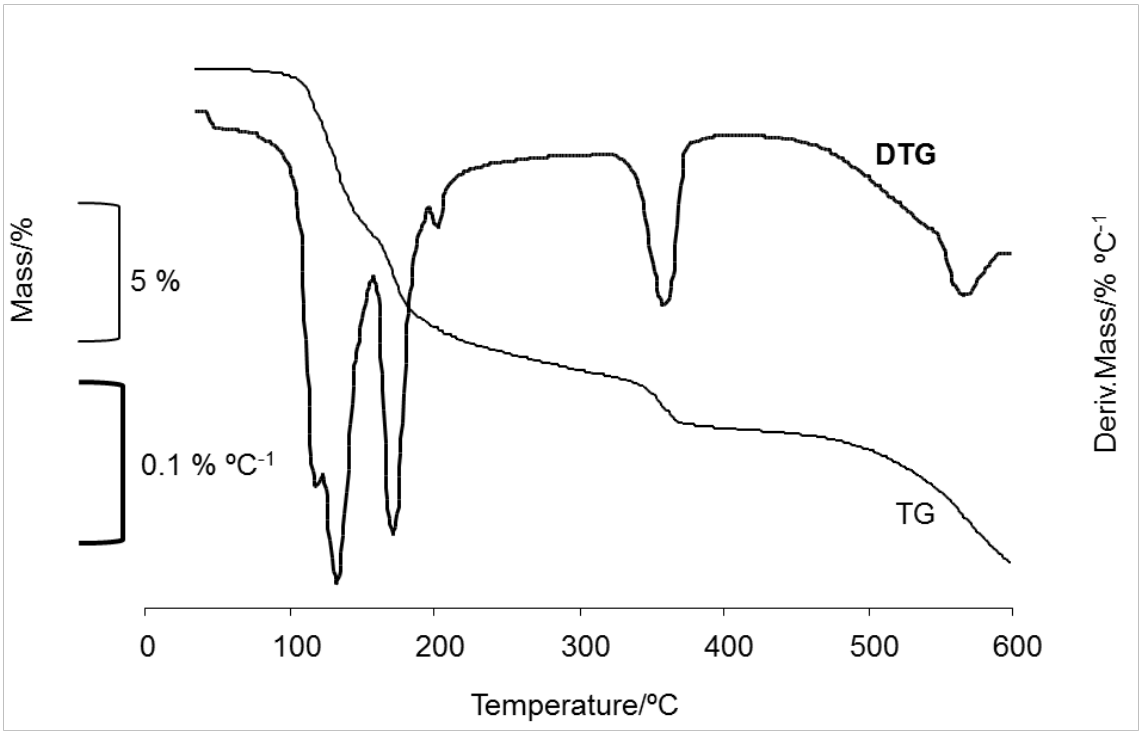

Fig. 9 TG and DTG curves of 10 % Zn (II) paste at 28 days of curing.

To summarize and to observe more clearly the effect of Zn (II) ions concentration in Portland cement pastes, in Figure 10, total mass loss values, M_T (from tables 3, 4 and 5) versus curing time have been represented. In 10 **a,** it can be seen that the behavior for paste with 0.1 % Zn (II) is very similar to the control paste, with a progressive increase in the total loss value due to the progress of cement hydration reaction. In the paste with 1 % Zn (II), a delay in the hydration reaction up to 3 days of curing is detected by the formation of Zn (II) compounds. However, from this age onwards the reaction proceeds as usual, as evidenced by the amount of Portlandite present in the paste which becomes equal to that contained in the control.

When the amount of Zn (II) increases (Figure 10 **b**), it can be observed that the delay in the hydration reaction is also confirmed by the total mass loss values below those corresponding to the control paste; in these cases Portlandite practically not formed during the curing times tested, the hydration of the cement is inhibited.

Total mass loss values remain nearly constant with curing time for each paste and increase as the concentration of Zn (II) is higher in the samples; this indicates that the higher the concentration of Zn (II), a greater number of compounds of Zn (II) are formed.

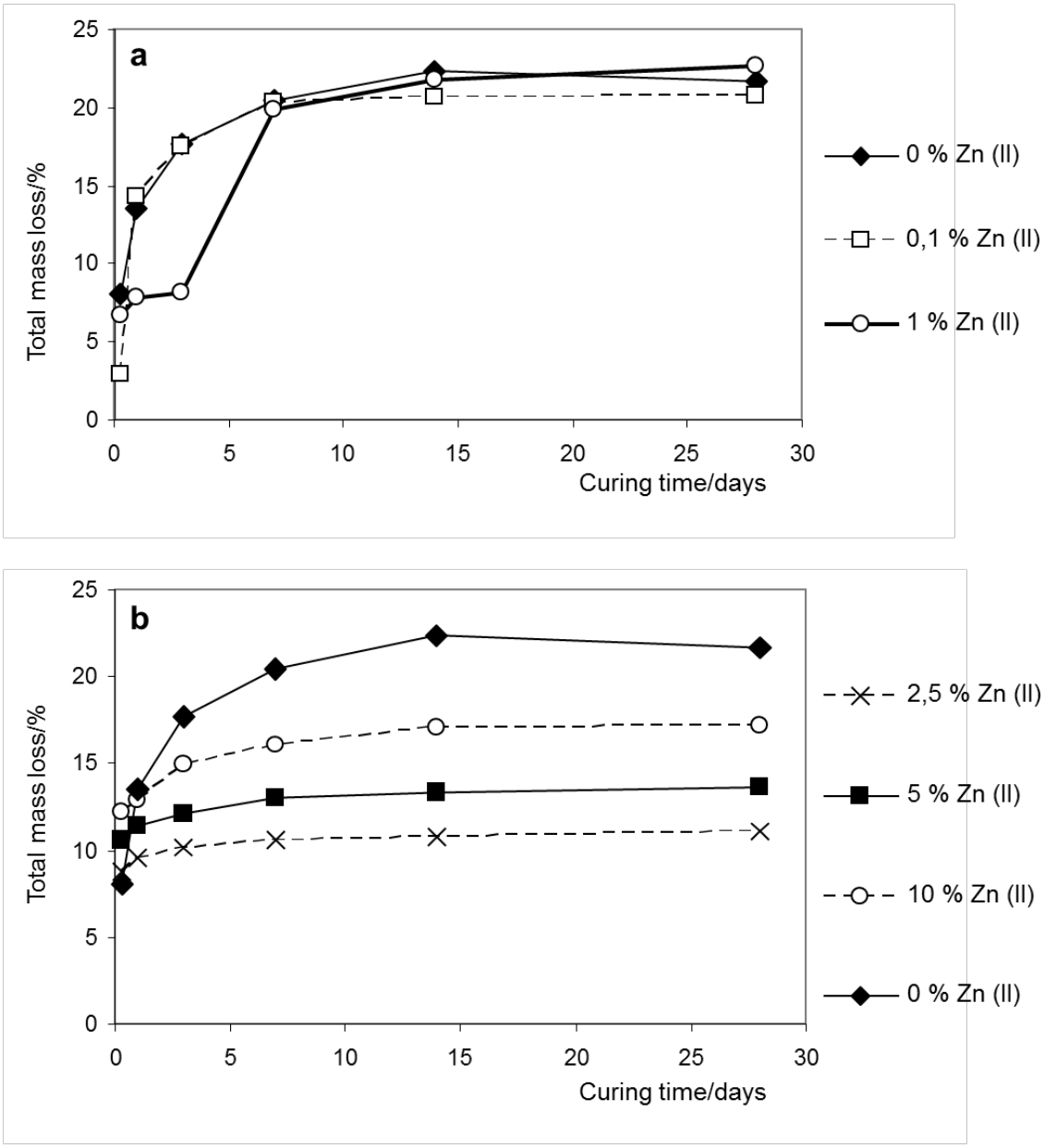

Fig. 10 Total mass loss values for the control paste and samples with different contents of Zn (II) versus time of curing.

3.3. SEM studies.

Scanning electron micrographs (SEM) of control paste are presented in figure 11 (as stated in paragraph 2, all SEM micrographs were made after 100 days of curing). In 11 **a,** a general vision of typical products of cement hydration is shown where clearly some hexagonal sheets of Portlandite can be identified; ettringite needles can also be observed in 11 **b**. Figure 11 **c** and **d** show two SEM micrographs of paste containing 1 % of Zn (II). In this case, hydration was advanced enough to produce the Portlandite that we can observe in both micrographs. In figure 11 **e,** (10 % of Zn (II) paste) it is evident the total absence of Portlandite over the particles examined. It appears a fibrous structure covering the entire surface of samples. Micrograph 11 **f** shows a detail of this structure that adopts the form of a ball. EXD analysis shows Ca (II) and Zn (II) as main metallic elements, and suggests the presence of $CaZn_2(OH)_6 \cdot 2H_2O$.

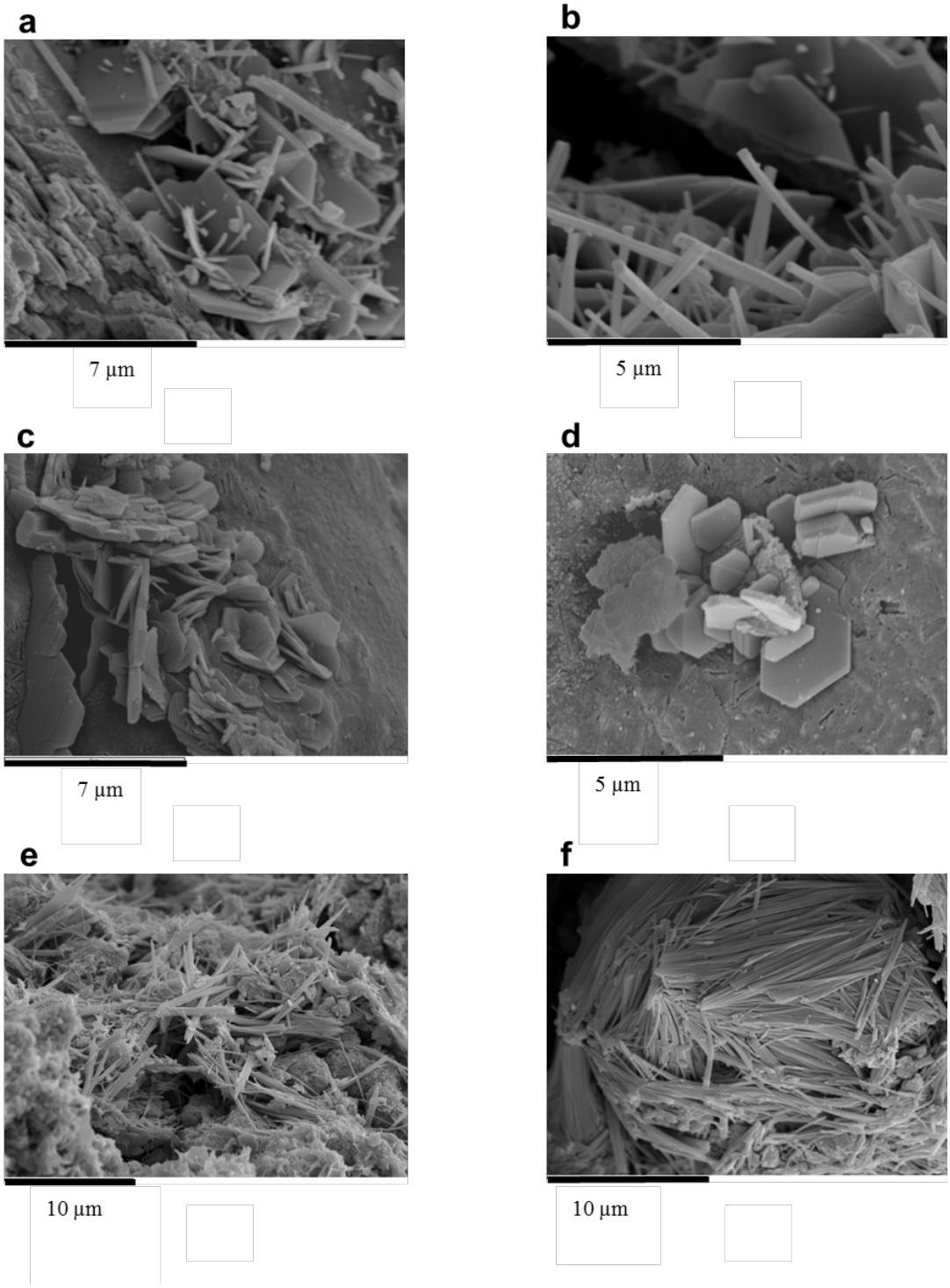

Fig. 11 SEM micrographs of **a** control paste (x8500), **b** control paste (x12000), **c** 1 % Zn (II) paste (x8000), **d** 1 % Zn (II) paste (x9000), **e** 10 % Zn (II) paste (x4000) and **f** 10 % Zn (II) paste (x5000) at 100 days' curing time.

3.4. Leaching studies.

Samples of pastes after 270 curing days were prepared for acid neutralization capacity (ANC) tests. Experimental results from ANC test of control and Zn (II) pastes are shown in figure 12. It can be observed the same behavior of samples depending on the amount of Zn (II) in the paste: when it increases, ANC values are lower. This behavior is logical because of the decrease in Portlandite content in the paste when increasing Zn (II) ions.

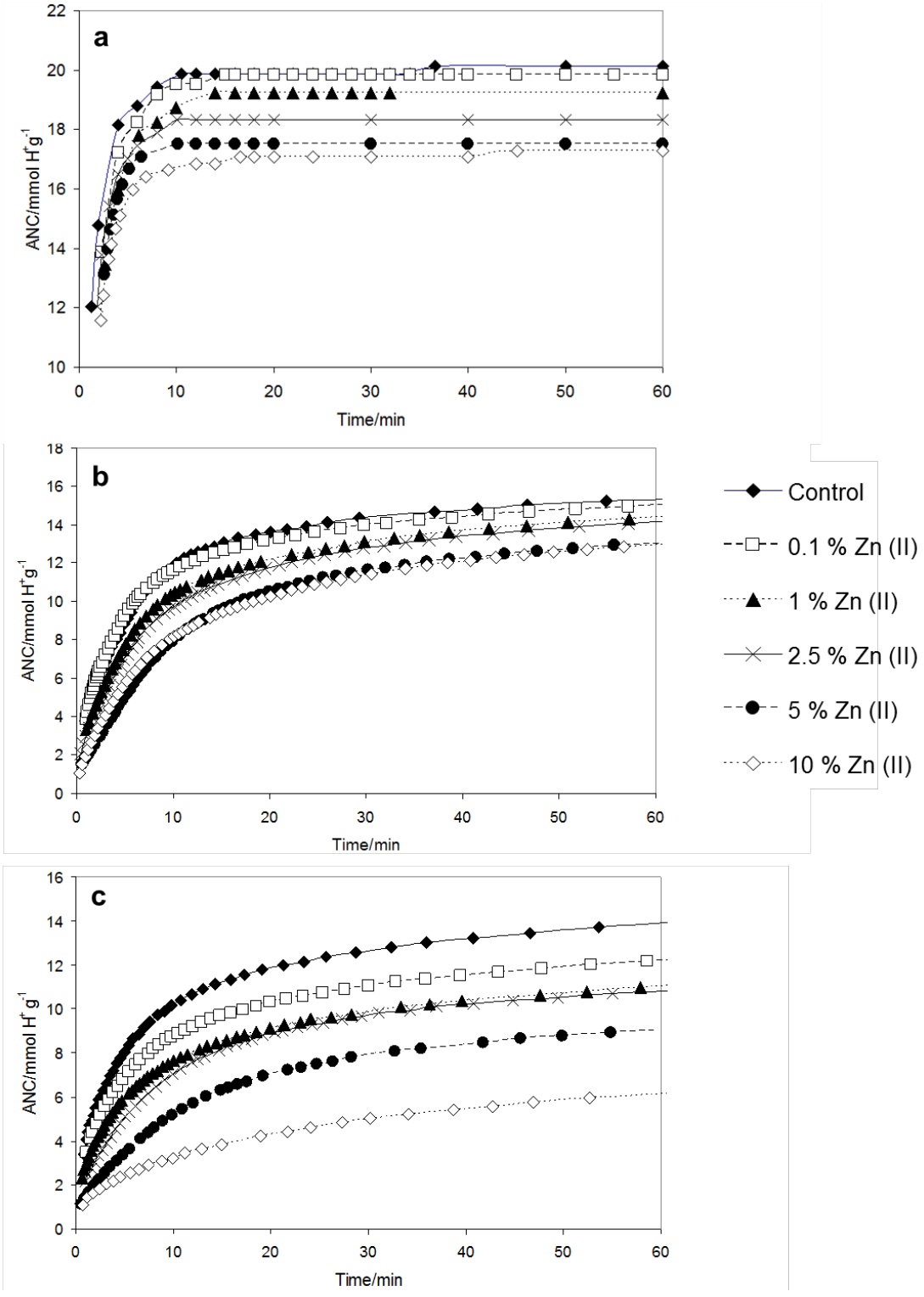

Fig. 12 ANC of control and Zn (II) pastes at **a** pH 2, **b** pH 4 and **c** pH 7.

For the experiments at pH 2, stabilization of ANC values was reached for all the samples before 20 minutes. At pH 4 and 7, the acid consumption was still increasing by the end of all the leaching tests, thus showing that the neutralization process was still activated at a small rate, whereas at pH 2 the neutralization had finished.

The amount of leached Zn (II) was determined by analyzing the Zn (II) ions content in the liquid phase after finishing the ANC tests. Figure 13 shows the released Zn (II) amount by unit mass of paste versus introduced Zn (II), at assayed pH. The amount leached at pH 7 is very low compared to that obtained at lower pH values.

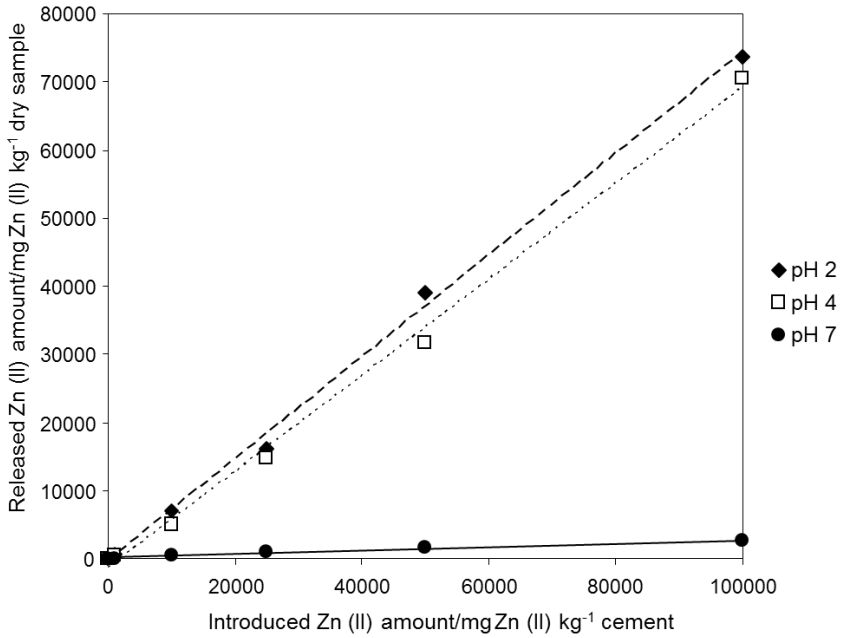

Fig. 13 Relation between leached Zn (II) and present Zn (II) in pastes at different pH values after finishing ANC tests.

3.5. Comparison of TG and leaching results.

Considering the results shown in sections 3.2. and 3.4., a correlation between the results of thermogravimetric analysis and the leaching studies can be established, already. Figure 14 shows ANC values of pastes containing different amounts of Zn (II) immobilized at pH assayed and at the last time of testing (60 minutes).

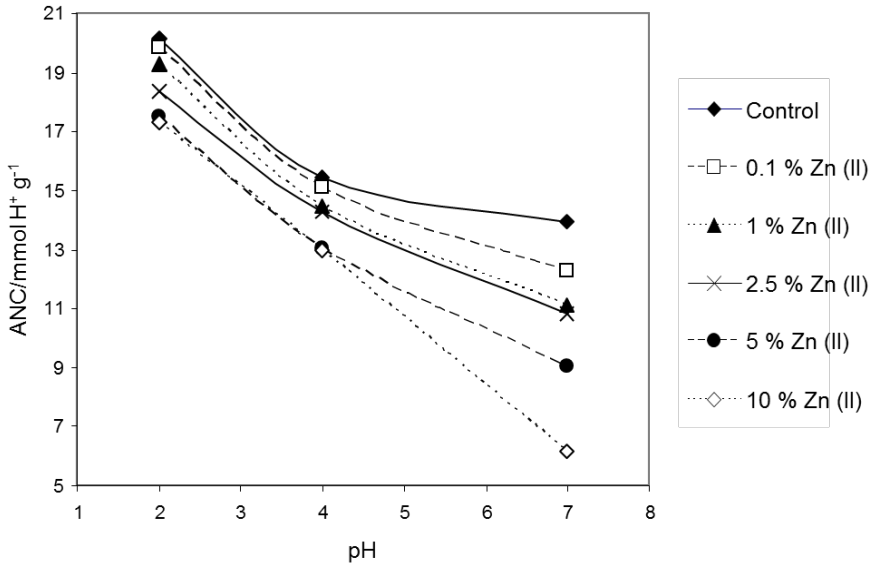

Fig. 14 ANC versus pH for control and Zn (II) pastes at 60 min.

It is evident that there is a decrease in ANC values in accordance with the increase in Zn (II) percentage in pastes. That confirms the conclusions obtained from thermogravimetric studies: the inhibition in the cement hydration reaction in presence of Zn (II) ions and the greater concentration of Zn (II), the more inhibition is produced.

Changes observed in CH peaks in DTG graphs of pastes containing Zn (II) evidence the consumption of OH^- ions from the low levels of Portlandite formed by Zn (II) ions immobilized, yielding new solid composites of Ca (II) and/or Zn (II). This fact implies a lesser amount of OH^- ions available to react with acid in ANC test, which is confirmed with the results presented in figure 14. The reason for this performance is the absorption and incorporation of calcium hydroxyzincate in the C-S-H matrix that prevents their further dissolution.

To find a correlation between thermogravimetric parameters and the results of leaching tests, we have related the parameters where the effect of Zn (II) ions in the paste is permanent and clearer. Thus, in figure 15 the total mass loss values (M_T) obtained by thermogravimetry in pastes with 1, 2.5, 5 and 10 % of Zn (II) at 7 hours, 1 and 3 days of curing versus the amount of Zn (II) leached (in pastes cured for 270 days) at pH 2 and pH 4, have been represented. A good logarithmic correlation has been found at the experimental conditions under which this experience has been performed. The correlation coefficients of the regression equations are shown in Table 7. This result is important because, in a preliminary approach, from a thermogravimetric analysis in a paste made in a few days of curing, it may allow us to estimate the amount of Zn (II) that could be leached, without costly and time-consuming tests. This result requires further research, considering other factors that may affect the hydration process.

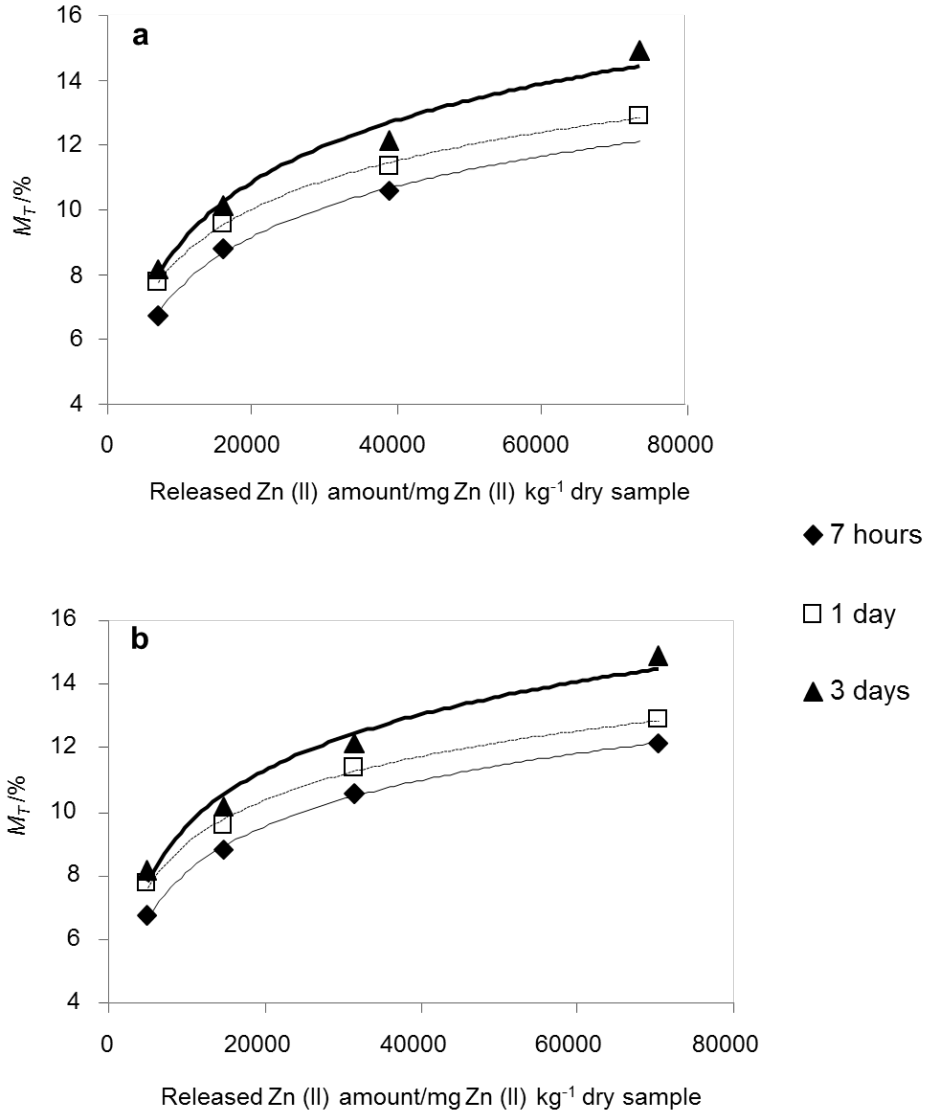

Fig. 15 Total loss values M_T of pastes with 1, 2.5, 5 and 10 % of Zn (II) at different curing times versus the amount of Zn (II) ions leached at **a** pH 2 and **b** pH 4.

$y = a \ln x - b$				
pH	Curing time	a	b	R^2
2	7 hours	21.472	11.241	0.999
	1 day	22.566	13.174	0.998
	3 days	2.758	16.471	0.976
4	7 hours	2.067	10.919	0.998
	1 day	1.963	9.060	0.995
	3 days	2.528	13.733	0.978
7	7 hours	2.728	9.575	0.963
	1 day	2.576	7.677	0.950
	3 days	3.271	11.630	0.910

Table 7 Correlations between total mass loss M_T and amount of leached Zn (II).

4. Conclusions.

- The consumption of OH^- ions by Zn (II) form hydrated calcium hydroxyzincate, $CaZn_2(OH)_6 \cdot 2H_2O$ mostly, which is deposited as a waterproof coating on the grains of C_3S delaying their hydration.
- Hydrated calcium hydroxyzincate has been identified as a major component formed by Zn (II) and OH^- ions. $Zn(OH)_2$ can also be detected in pastes containing Zn (II) ions higher than 1 % ; in addition, $Zn_5(CO_3)_2(OH)_6$ and $ZnCO_3$ appear for pastes containing more than 2.5 % Zn (II).
- TG and XRD results confirm the absence of Portlandite for short curing times (less than 3 days), which explains the delay in the setting due to the consumption of OH^- ions by the Zn (II) ions in the initial stage of cement hydration.
- ANC values of pastes decreases when the amount of Zn (II) increases because of the consumption of OH^- ions by Zn (II), which form insoluble compounds, probably due to the incorporation of these compounds into hydrated calcium silicates.
- A correlation between total mass loss (M_T in TG analysis) and leached Zn (II) ions in long term curing pastes was established. This result is important because, in a preliminary approach from a thermogravimetric analysis on an early-aged cement paste containing Zn (II) ions, an estimation of the amount of Zn (II) that could be leached can be carried out.

Acknowledgement

We would like to thank the Unit of Microscopy at the Universitat Politècnica de València and we also want to thank Lourdes Aznar for providing language help in the English version of this paper.

References

[1] Mojumdar S.C., Sain M., Prasad R.C., Sun L., Venart J.E.S. Selected thermoanalytical methods and their applications from medicine to construction, Part I. Journal of Thermal Analysis and Calorimetry 2007; 90:653–662.

[2] Perraki M., Perraki T., Kolovos K., Tsivilis S., Kakali G. Secondary raw materials in cement industry. Evaluation of their effect on the sintering and hydration processes by thermal analysis. Journal of Thermal Analysis and Calorimetry 2002; 70:143-150.

[3] Neves A., Dias Toledo R., de Moraes Rego E., Dweck J. Early stages hydration of high initial strength Portland cement. Part I. Thermogravimetric analysis on calcined mass basis. Journal of Thermal Analysis and Calorimetry 2012; 108:725-731, DOI: 10.1007/s10973-012-2256-z.

[4] Balek V., Bydžovský J., Dufka A., Drochytka R., Beckman I.N. Use of emanation thermal analysis to characterize microstructure development during Portland cement hydration. Journal of Thermal Analysis and Calorimetry 2012; DOI: 10.1007/s10973-012-2314-6.

[5] Zhang Q., Ye G. Dehydration kinetics of Portland cement paste at high temperature. Journal of Thermal Analysis and Calorimetry 2012; DOI: 10.1007/s10973-012-2303-9.

[6] Menéndez E., Vega L., Andrade C. Use of decomposition of portlandite in concrete fire as indicator of temperature progression into the material. Application to fire-affected builds. Journal of Thermal Analysis and Calorimetry 2012; DOI: 10.1007/s10973-011-2159-4.

[7] Galan I., Andrade C., Castellote M. Thermogravimetrical analysis for monitoring carbonation of cementitious materials. Uptake of CO2 and deepening in C–S–H knowledge. Journal of Thermal Analysis and Calorimetry 2012; DOI: 10.1007/s10973-012-2466-4.

[8] Batchelor B. Overview of waste stabilization with cement. Waste Management 2006; 26:689-698.

[9] Gineys N., Aouad G., Damidot D. Managing trace elements in Portland cement – Part I: Interactions between cement paste and heavy metals added during mixing as soluble salts. Cement & Concrete Composites 2010; 32:563-570.

[10] Erdem M., Özverdi A. Environmental risk assessment and stabilization/solidification of zinc extraction residue: II. Stabilization/solidification. Hydrometallurgy 2011; 105:270-276.

[11] Nocuń-Wczelik W., Małolepszy J. Application of calorimetry in studies of the immobilization of heavy metals in cementitious materials. Thermochimica Acta 1995; 269/270:613-619.

[12] Dweck J., Buchler P.M., Cartledge F.K. The effect of different bentonites on cement hydration during solidification/stabilization of tannery wastes. Journal of Thermal Analysis and Calorimetry 2001; 64:1011-1016.

[13] Melchert M.B.M., Viana M.M., Lemos M.S., Dweck J., Buchler P.M. Simultaneous solidification of two catalyst wastes and their effect on the early stages of cement hydration. Journal of Thermal Analysis and Calorimetry 2011; 105:625-633.

[14] Vessalas K., Thomas P.S., Ray A.S., Guerbois J.P., Joyce P., Haggman J. Pozzolanic reactivity of the supplementary cementitious material pitchstone fines by thermogravimetric analysis. Journal of Thermal Analysis and Calorimetry 2009; 97:71-76.

[15] Tommaseo C.E., Kersten M., Aqueous Solubility Diagrams for Cementitious Waste Stabilization Systems. 3. Mechanism of Zinc Immobilization by Calcium Silicate Hydrate. Environmental Science and Technology 2002; 36:2919-2925 .

[16] Peyronnard O., et al. Study of mineralogy and leaching behavior of stabilized/solidified sludge using differential acid neutralization analysis. Cement and Concrete Research 2009; doi:10.1016/j.cemconres.2009.03.016.

[17] Moulin I. et al. Lead, zinc and chromium (III) and (VI) speciation in hydrated cement phases. International Conference on the Science and Engineering of Recycling for Environmental Protection, Waste Materials in Construction (WASCON 2000), Harrogate, England, 2000, pp. 269-280.

[18] Ziegler F., Gieré R., Johnson C.A. Sorption Mechanisms of Zinc to Calcium Silicate Hydrate: Sorption and Microscopic Investigations. Environmental Science and Technology 2001; 35:4556-4561.

[19] Qiao X.C., Poon C.S., Cheeseman C.R. Investigation into the stabilization/solidification performance of Portland cement through cement clinker phases. Journal of Hazardous Materials 2007; B139:238-243.

[20] Chen Q.Y. et al. Immobilisation of heavy metal in cement-based solidification/stabilisation: A review. Waste Management 2009; 29:390-403.

[21] Chen Q.Y. et al. Characterisation of products of tricalcium silicate hydration in the presence of heavy metals. Journal of Hazardous Materials 2007; 147:817-825.

[22] Fernandez-Olmo I., Chacon E., Irabien A. Influence of lead, zinc, iron (III) and chromium (III) oxides on the setting time and strength development of Portland cement. Cement and Concrete Research 2001; 31:1213-1219.

[23] Fernandez-Olmo I., Chacon E., Irabien A. Leaching Behavior of Lead, Chromium (III) and Zinc in Cement/Metal Oxides Systems. Journal of Environmental Engineering © ASCE 2003; June:532-538.

[24] Cappuyns V., Swennenb R. The application of pHstat leaching tests to assess the pH-dependent release of trace metals from soils, sediments and waste materials. Journal of Hazardous Materials 2008; 158:185-195.

[25] Payá J., Monzó J., Borrachero M.V., Velázquez S. Evaluation of the pozzolanic activity of fluid catalytic cracking catalyst residue (FC3R): Thermogravimetric analysis studies on FC3R-Portland cement pastes. Cement and Concrete Research 2003; 33:603-609.

[26] Wang S., Yang Z., Zeng L. Study of calcium zincate synthesized by solid-phase synthesis method without strong alkali. Materials Chemistry and Physics 2008; 112:603-606.

[27] Stumm A. et al. Incorporation of zinc into calcium silicate hydrates, Part I: formation of C-S-H(I) with C/S=2/3 and its isochemical counterpart gyrolite. Cement and Concrete Research 2005; 35:1665-1675.

[28] Stephan D., Mallmann R., Knöfel D., Härdtl R. High intakes of Cr, Ni, and Zn in clinker, Part II. Influence on the hydration properties. Cement and Concrete Research 1999; 29:1959-1967.

[29] Liu Y. et al. Thermal decomposition of basic zinc carbonate in nitrogen atmosphere. Thermochimica Acta 2004; 414:121-123.

[30] Wahab R. et al. Synthesis and characterization of hydrozincite and its conversion into zinc oxide nanoparticles. Journal of Alloys and Compounds 2008; 461:66-71.

[31] Hatakeyama T. and Liu Z. Handbook of Thermal Analysis, Wiley; 2000.